REPORT DOCUMENTATION PAGE

Form Approved OMB NO. 0704-0188

1. REPORT DATE (DD-MM-YYYY)	2. REPORT TYPE	3. DATES COVERED (From - To)
	New Reprint	-

4. TITLE AND SUBTITLE
Multifunctional ultra-high vacuum apparatus for studies of the interactions of chemical warfare agents on complex surfaces

5a. CONTRACT NUMBER
W911NF-09-1-0150

5b. GRANT NUMBER

5c. PROGRAM ELEMENT NUMBER
611102

6. AUTHORS
Amanda R. Wilmsmeyer, Wesley O. Gordon, Erin Durke Davis, Brent A. Mantooth, Teri A. Lalain, John R. Morris

5d. PROJECT NUMBER

5e. TASK NUMBER

5f. WORK UNIT NUMBER

7. PERFORMING ORGANIZATION NAMES AND ADDRESSES
Virginia Polytechnic Institute & State Unive
North End Center, Suite 4200
300 Turner Street, NW
Blacksburg, VA 24061 -0001

8. PERFORMING ORGANIZATION REPORT NUMBER

9. SPONSORING/MONITORING AGENCY NAME(S) AND ADDRESS (ES)
U.S. Army Research Office
P.O. Box 12211
Research Triangle Park, NC 27709-2211

10. SPONSOR/MONITOR'S ACRONYM(S)
ARO

11. SPONSOR/MONITOR'S REPORT NUMBER(S)
55374-CH.19

12. DISTRIBUTION AVAILIBILITY STATEMENT
Approved for public release; distribution is unlimited.

13. SUPPLEMENTARY NOTES
The views, opinions and/or findings contained in this report are those of the author(s) and should not contrued as an official Department of the Army position, policy or decision, unless so designated by other documentation.

14. ABSTRACT
A fundamental understanding of the surface chemistry of chemical warfare agents is needed to fully predict the interaction of these toxic molecules with militarily relevant materials, catalysts, and environmental surfaces. For example, rules for predicting the surface chemistry of agents can be applied to the creation of next generation decontaminants, reactive coatings, and protective materials for the warfighter. Here, we describe a multifunctional ultra-high vacuum instrument for conducting comprehensive studies of the adsorption, desorption, and surface chemistry of chemical warfare agents

15. SUBJECT TERMS
Surface Science, CWA, XPS, FTIR, TPD, ultrahigh vacuum, mass spectrometry, agents

16. SECURITY CLASSIFICATION OF:			17. LIMITATION OF ABSTRACT	15. NUMBER OF PAGES	19a. NAME OF RESPONSIBLE PERSON
a. REPORT	b. ABSTRACT	c. THIS PAGE			John Morris
UU	UU	UU	UU		19b. TELEPHONE NUMBER: 540-231-2472

Report Title

Multifunctional ultra-high vacuum apparatus for studies of the interactions of chemical warfare agents on complex surfaces

ABSTRACT

A fundamental understanding of the surface chemistry of chemical warfare agents is needed to fully predict the interaction of these toxic molecules with militarily relevant materials, catalysts, and environmental surfaces. For example, rules for predicting the surface chemistry of agents can be applied to the creation of next generation decontaminants, reactive coatings, and protective materials for the warfighter. Here, we describe a multifunctional ultra-high vacuum instrument for conducting comprehensive studies of the adsorption, desorption, and surface chemistry of chemical warfare agents on model and militarily relevant surfaces. The system applies reflection-absorption infrared spectroscopy, x-ray photoelectron spectroscopy, and mass spectrometry to study adsorption and surface reactions of chemical warfare agents. Several novel components have been developed to address the unique safety and sample exposure challenges that accompany the research of these toxic, often very low vapor pressure, compounds. While results of vacuum-based surface science techniques may not necessarily translate directly to environmental processes, learning about the fundamental chemistry will begin to inform scientists about the critical aspects that impact real-world applications.

REPORT DOCUMENTATION PAGE (SF298)
(Continuation Sheet)

Continuation for Block 13

ARO Report Number 55374.19-CH
Multifunctional ultra-high vacuum apparatus for s...

Block 13: Supplementary Note

Approved for public release; distribution is unlimited.

Multifunctional ultra-high vacuum apparatus for studies of the interactions of chemical warfare agents on complex surfaces

Amanda R. Wilmsmeyer,[1] Wesley O. Gordon,[2] Erin Durke Davis,[3] Brent A. Mantooth,[2] Teri A. Lalain,[2] and John R. Morris[1]
[1]*Department of Chemistry, Virginia Tech, Blacksburg, Virginia 24061, USA*
[2]*Research and Technology Directorate, U.S. Army Edgewood Chemical Biological Center, Aberdeen Proving Ground, Maryland 21010, USA*
[3]*OptiMetrics, Inc., Abingdon, Maryland 21009, USA*

(Received 19 September 2013; accepted 26 November 2013; published online 2 January 2014)

A fundamental understanding of the surface chemistry of chemical warfare agents is needed to fully predict the interaction of these toxic molecules with militarily relevant materials, catalysts, and environmental surfaces. For example, rules for predicting the surface chemistry of agents can be applied to the creation of next generation decontaminants, reactive coatings, and protective materials for the warfighter. Here, we describe a multifunctional ultra-high vacuum instrument for conducting comprehensive studies of the adsorption, desorption, and surface chemistry of chemical warfare agents on model and militarily relevant surfaces. The system applies reflection-absorption infrared spectroscopy, x-ray photoelectron spectroscopy, and mass spectrometry to study adsorption and surface reactions of chemical warfare agents. Several novel components have been developed to address the unique safety and sample exposure challenges that accompany the research of these toxic, often very low vapor pressure, compounds. While results of vacuum-based surface science techniques may not necessarily translate directly to environmental processes, learning about the fundamental chemistry will begin to inform scientists about the critical aspects that impact real-world applications.
 [http://dx.doi.org/10.1063/1.4846656]

I. INTRODUCTION

Detailed knowledge about the interfacial chemistry and physics of chemical warfare agents (CWAs) is critical to developing a fundamental understanding of the processes that influence the effectiveness of decontamination,[1–8] protection,[3,9] and sensing[4,9–11] technologies as well as to accurately predict environmental fate[12–15] of agents. Unfortunately, little is known about the mechanisms, rates, and probabilities of agent-surface adsorption, diffusion, and reactions. For example, fundamental knowledge of how the surface functionality of military paints and coatings impacts chemical resistance would enable the fine-tuning of the surface to improve performance. However, many surface sensitive methods can be expensive and challenging to implement, particularly for complex military materials. This problem is compounded by the cost, safety, and legal challenges of working with super toxic chemicals. As a result, a large body of existing work has focused on exploring the surface chemistry of CWA simulants (less toxic analogues of the agents), rather than the live agents.[16–30] While direct comparisons between agents and simulants have been made through computational studies, little experimental data exist for the development of agent-simulant correlations. The instrumentation described here is focused on advancing knowledge about the surface chemistry of highly toxic compounds in a way that will empower improvements in technologies and methods to mitigate the threat of chemical warfare or chemical terrorism.

While surface sensitive chemical studies of simulant adsorption and reaction are now common,[31] few surface science focused studies of the agents have been conducted. One of the initial reports of the surface chemistry of live chemical agents was provided by Vanbokhoven *et al.*[32–34] Their work focused on studies of the reaction kinetics of sarin on gamma alumina surfaces. This work was followed by other investigations of organophosphate CWA decomposition on alumina.[35] In addition, Wagner and colleagues employed solid state NMR to study the decomposition of CWAs on MgO,[36] AgY and NaY zeolites,[37] CaO,[38] and Al_2O_3.[39] More recently, the decomposition of sarin on Al_2O_3 nanoparticles[40] was studied by attenuated total reflectance (ATR) Fourier transform infrared (FTIR) spectroscopy and the desorption of sarin from silica surfaces was investigated via reverse gas phase chromatography.[41] This body of work, while valuable, is limited in its ability to simultaneously track surface-bound and gas-phase reaction products in a way that provides overall reaction rates on surfaces that are well characterized with surface-sensitive methods such as photoelectron spectroscopy. Moreover, most of the published studies that employ actual CWAs have been conducted in solution or under atmospheric conditions,[36,37,42–44] which preclude the application of surface analytical instrumentation. Here, we describe the design, construction, and testing of a novel multi-functional ultra-high vacuum (UHV) instrument for study of the surface interactions and chemistries of live CWAs on model and actual military surfaces.

The UHV instrument combines vacuum compatible chemical dosing methods with reflection absorption infrared spectroscopy (RAIRS), mass spectrometry (MS), and x-ray photoelectron spectroscopy (XPS) to probe the surface chemistry of CWAs. The ability to cool or heat samples enables

observation over the full range of thermally driven events from adsorption to desorption or reaction. Due to the hazardous nature and unique handling requirements of the chemicals involved, novel dosing and safety features were developed and integrated into the overall instrument to ensure worker safety. In Sec. II we describe the instrument in general terms, and the requirements that were used for the final instrument design. We then provide a detailed description of each component. In Sec. III, we demonstrate the instrumental capabilities through an initial study into the adsorption of simulants and live CWAs on model particulate surfaces.

II. INSTRUMENT DESIGN

A. Overview and design criteria

One of our primary objectives was to design and construct a surface science instrument capable of characterizing the chemistry of extremely toxic chemical warfare agents in one integrated system. Therefore, we constructed a UHV surface science apparatus (Fig. 1) capable of *in situ* vibrational spectroscopy to track the breaking and formation of surface bonds during exposure of a sample to an agent of interest while, at the same time, monitoring the emergence of gas-phase products from the surface. These goals were accomplished by combining precision vapor dosing capabilities through a custom-designed source for CWAs, a doubly differentially pumped mass spectrometer, and reflection (or transmission) Fourier-transform infrared spectroscopy. These methods afford the simultaneous monitoring of surface-bound and gas-phase products during a reaction. Pre and post surface elemental analysis is performed in this system with an x-ray photoelectron spectrometer and temperature-programmed desorption (TPD) methods.

Although many of the instruments incorporated into the system are standard surface analytical tools, the safety challenges posed by conducting experiments with live chemical warfare agents required several unique design considerations: (1) The surface sample introduction and removal load-lock system must be completely contained within a custom chemical hood that is regularly inspected and certified for CWA operations; (2) All roughing and backing pumps, along with every exhaust line, must be fully contained within engineering controls and vent to filters appropriate for CWA work; (3) Exposure of a surface to an agent of interest must be accomplished from a source containing no more than microgram quantities of agent that is fully contained within the chemical hood or the UHV chamber at all times; (4) The chamber must be decontaminated via hot gas and pumping cycles prior to removal of any flange; and (5) The entire chamber must be maintained under negative pressure during maintenance with the exhaust properly filtered. The apparatus that was designed and constructed to meet these requirements is shown schematically in Fig. 1. Table I provides the key experimental and safety requirements of the instrument along with how they were accomplished. Below, we highlight several of the most critical and novel features of the apparatus.

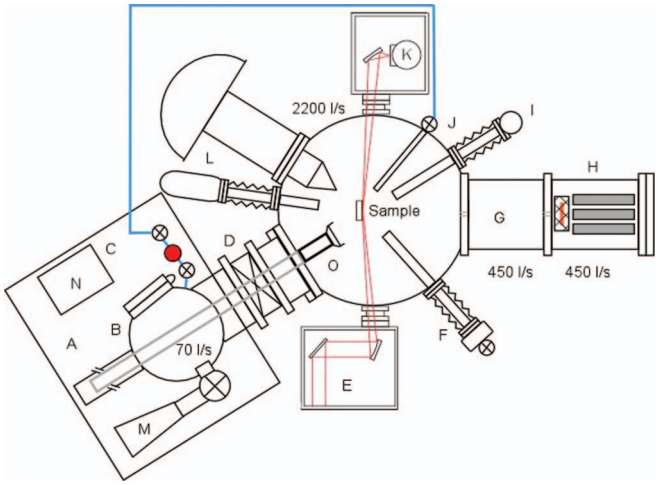

FIG. 1. Schematic (not to scale) of the UHV system showing the primary equipment. (A) transfer arm, (B) load lock chamber and pump, (C) chemical agent vapor dose manifold, (D) gate valve, (E) IR light entrance optics, (F) capillary array doser, (G) apertures and differential pumping stage, (H) mass spectrometer chamber and pump, (I) cryostat for solid sorbent doser, (J) directional agent vapor doser, (K) IR light exit optics and detector, (L) XPS system and ion gun, (M) Venturi tube ventilation system, (N) foreline pumps for all the turbomolecular pumps.

B. Chamber construction, pumping, and safety

The central instrumental scaffold is a custom designed multiport 23 L UHV chamber constructed out of 316 L stainless steel (SS) with all ports equipped with con-flat® flanges (Kurt J. Lesker Company (KJLC)). The chamber is evacuated by a 2200 L/s magnetically levitated turbomolecular pump (A2200C, Edwards Vacuum), which can be isolated

TABLE I. Design requirements and approach (letters correspond to Fig. 1).

Design requirement	Experimental approach
Dynamic pressure range: 10^{-9} to 10^{-2} Torr	2200 L/s main turbo with variable speed and gate valve
Contained rapid sample introduction	Load-lock transfer system coupled to chemical hood (B)
Precision CWA dosing with μg quantities	*In vacuo* solid sorbent dosing system (O coupled to I)
Pre and post surface characterization	TPD (H), FTIR (E, K), and spatially resolved XPS (L)
Controlled surface temperature and position	Precision manipulator with heater and LN_2 cooling
Gas-phase product identification	Quadrupole mass spectrometer (H)
In situ monitoring of surface adsorbates	Reflection or transmission FTIR (E, K)
Mass analysis of surface adsorbates	Temperature-programmed desorption (H)
Reaction probability measurements	Line-of-sight uptake probability measurements (H)
Kinetics measurements	Time-resolved IR and mass spectrometry (E, K, and H)
CWA-contaminated exhaust handling	All metal seals, foreline pumps vent into chemical hood (A, B, N)

from the main chamber by a 12 in. gate valve (KJLC). This pump is backed by an oil-free scroll pump (Edwards XDS-35). The turbomolecular pump was chosen for this system because of its high pumping speed and significant compression ratio for mid-sized organic molecules, such as CWAs. These pumping characteristics are critical for performing experiments under high gas flux conditions. In addition, the pumping speed can be varied by reducing the rotation speed of the turbines, thereby enabling experiments to be performed under low-vacuum conditions. Finally, this pump cleanly removes gases from the chamber through a foreline pump located within a controlled environment, ensuring that agent vapors are quickly and continually exhausted to the hood and away from the laboratory personnel.

The chamber is designed to allow multiple bake-out cycles and hot gas purges to eliminate residual CWA contamination that may exist following a study. These cycles are accomplished by encasing the system in a custom-designed thermal tent equipped with a controlled heating system (Hemi Heating, Inc.). The tent and associated heaters provide even distribution of heat throughout the system. The chamber can be heated to 373 K at a rate of $\sim$ 0.2 K/min and then held at that temperature, under vacuum, for extended periods of time. While heating, the chamber can be scrubbed by introducing N_2 or CO_2 through an auxiliary dosing line. Several fill-evacuation cycles effectively reduce chamber contamination, as monitored by the mass spectrometer and XPS analysis of test sorbent materials that are positioned within the main chamber during chamber cleaning. A tool has also been developed to enable solvent-wetted swab samples to be collected on chamber walls to confirm decontamination prior to maintenance. Briefly, a polyurethane foam swab (Techspray P/N 2302-50) is wetted with 5 mL of isopropyl alcohol, attached to the reach in tool, and wiped over $\sim$10 cm^2 of chamber surface. The absorbed material is extracted from the swab in isopropyl alcohol (10 mL) and analyzed via liquid chromatography-mass spectrometry, which is sensitive to lower than 0.1 monolayer quantities of chemical agent on the chamber surface.

Because the chamber can be coupled to high-pressure gas cylinders for cleaning cycles and other surface chemistry experiments, there exists a remote danger of inadvertent over-pressurization of the system. Over-pressurization may occur, for example, if a regulator were to fail while the pumping system was isolated. In addition, there is a liquid nitrogen reservoir contained within the main chamber to cool the sample holder, which also poses an over-pressurization danger in the event that one of the liquid nitrogen feed lines were to fail. Over-pressurization of a closed system can cause catastrophic failure of the chamber resulting in injury or exposure of laboratory personnel to hazardous chemicals. To mitigate this risk, a custom-designed ASTM-certified burst disk assembly (MDC Vacuum) was incorporated into the system. In this design, a standard conflat-flanged UHV burst disk was welded to a conflat half-nipple and connected to metal hosing which exhausts into the chemical hood system. In the event of over-pressurization, the disk will burst and the vapor will be directed into the hood where it exhausts from the laboratory through surety (certified for agent use) filters.

In any UHV surface science system, regular instrument maintenance is required to keep components operating properly and to make repairs on malfunctioning components. Maintenance for this system is accomplished by first performing several cycles of hot-gas cleaning followed by MS and XPS analysis to verify the general safety of the system. However, the complete absence of trace amounts of CWAs from the system is never guaranteed. Therefore, prior to venting the chamber and opening a flange, the chamber is vented with ultra-high purity N_2 to slightly below atmospheric pressure, then the main chamber is opened to the load-lock chamber, which is located inside of the surety hood. The load lock chamber is coupled to a 1500 cfm Venturi blower (McMaster-Carr). This design provides a constant negative pressure inside the vacuum chamber and is operated continually while the system is open to atmosphere. Laboratory air is continually pulled through any open flange through the main and auxiliary chambers and exhausted into the surety hood. In this way, residual vapors do not escape the system during system maintenance. Continual sampling and monitoring of the laboratory air ensures the safety of laboratory personal during maintenance as well as during normal operation of the system.

The system pressures, temperatures, and pump status are continuously monitored through a custom-built interlock system with electromagnetic switches, National Instruments (NI) Fieldbus hardware for communication and control, and manual 3-way control switches. In the event of a power outage, loss of communication with the control computer, a pressure excursion, or loss of pressurized air for the pneumatic valves, all valves are closed and pumps turned off. A battery backup enables the computer to maintain operation of pumps and valves in the event of short power interruptions. The 3-way switches allow for manual override if needed for maintenance or troubleshooting. All equipment is controlled using custom NI LabView® software to control instrumentation, collect and log data from gauges and other sensors, and to prevent accidental operation of sensitive equipment under high pressure conditions.

C. Surface sample manipulator and transfer

Surface samples are introduced into the UHV chamber via a load-lock system that is coupled to the surety chemical fume hood adjacent to the main chamber. The load-lock chamber itself resides inside the hood and is connected to the main UHV chamber through an air-tight seal around a 4 in. tube. The location of the load-lock chamber inside of the hood enables the safe and efficient introduction or removal of samples to and from the main chamber. Inside of the hood, the spherical load-lock chamber is evacuated by a 70 L/s turbomolecular pump (Pfeiffer) backed by a scroll pump (Edwards Vacuum, nXDS6iC). A gate valve (KJLC) separates the load lock from the UHV chamber, and a linear, magnetically coupled rotary transfer arm with one meter of travel is used for sample handling and transfer (MDC Vacuum). A load lock gimbal is used to ensure proper alignment of the sample mount with the docking receptacle on the manipulator.

Surface samples are mounted onto a molybdenum platen, which is in turn secured onto the linear transfer arm via a spring-loaded fork (customized STLC transfer system, Thermionics Inc.). Once the load-lock chamber is evacuated, the isolation gate valve is opened and the sample is transferred into the main chamber where it mates with the receiver on the manipulator. The precision sample manipulator provides 6 cm of travel in the plane of the gas source and detectors, 20 cm of vertical travel, 360° of rotation, and tilting capabilities in the X and Y directions. The removable platen can accommodate panels of military paint samples, polymeric materials, or any other vacuum compatible sample up to 30 mm in diameter and 4 mm in thickness. The sample can be heated up to 1000 K via resistive heating of tungsten filaments behind the sample platen and is controlled with an integrated power supply coupled to a proportional–integral–derivative controller. Liquid cooling enables sample temperatures as low as 100 K, when using cryogenic fluids. The sample platen also includes a transferrable type K thermocouple for measuring surface temperature, while a second thermocouple spot welded to the mount provides an independent reference temperature reading. The sample platen is electrically isolated from the chamber but is in contact with an electrical feedthrough to enable biasing or measuring of ion current on electrically conducting samples.

D. Effusive gas sources

Once the samples are mounted onto the manipulator, they are laser-aligned such that they are positioned at the focal point of the three effusive gas sources, the infrared spectrometer, and the quadruple mass spectrometer. Two dosers have been designed especially for handing extremely toxic CWAs, with either high or low vapor pressures. The requirements for CWA dosers are threefold: (1) the CWAs remain contained within the surety hood or the UHV chamber at all times, (2) the quantity of agent employed in the dosing must be on the microgram scale, and (3) dosing should be performed *in situ* with FTIR and mass spectrometric measurements. These design requirements were met by using a solid sorbent doser and a directional vapor doser.

1. Solid sorbent doser

The CWA solid sorbent doser (Fig. 2) was designed specifically for dosing low vapor pressure molecules. This doser is based on a transferrable, sealable, solid-sorbent-containing cartridge (Fig. 2, No. 2) that can be charged with agent while inside the surety hood. All of the cartridge components are machined from 400 series, magnetic stainless steel. Much of the stainless steel cartridge is bored to retain a solid sorbent material for the physisorption of agent. The cartridge, once charged with agent, is sealed via a reverse-threaded o-ring sealed cap (Fig. 2, No. 3) and mounted onto the linear translator transfer arm (Fig. 2, No. 4) inside of the load-lock chamber. The mating of the sealed cartridge to the transfer arm is secured with two alignment posts on the cartridge and two rare earth magnets press fit into the transfer arm adapter. Following evacuation, the load-lock chamber is opened to the main chamber and the sorbent cartridge is translated through the main chamber (with the surface sample raised out of the path of the translator) and mounted via clockwise rotation onto the variable temperature UHV cryostat (Janis, ST-400) capable of operation from 80 to 500 K. Once mounted onto the cryostat receiver (Fig. 2, No. 1), the transfer arm is removed and the cartridge assembly is cooled well below the sublimation temperature of the CWA. Once cooled, the cap can be removed (via clockwise rotation of the linear rotatable transfer arm) when one is ready to begin an experiment. Following removal of the cap, the surface sample can be re-positioned into the line-of-sight of the doser. Then, the doser is translated forward to within 1/8 in. of the sample and is heated until the CWA desorbs from the sorbent material within the cartridge. As the molecules desorb from the cartridge, they impinge on the surface sample and the uptake is monitored with the FTIR. To remove the cartridge, the transfer arm adapter-cap assembly, is aligned with the cartridge and the arm is rotated counter-clockwise. This rotation begins to screw the cap back on then unscrews the cartridge from the cryostat. The cartridge can then safely be removed from the main chamber and preparations can be made for the next experiment. In this way, the entire lifespan of the cartridge, sorbent, and agent is spent either within the surety hood or the main UHV chamber. The solid sorbent doser has been successfully used to dose a surface sample with the chemical agent VX (*O*-ethyl *S*-[2-(diisopropylamino)ethyl] methylphosphonothioate using an initial volume of $<10\ \mu$L.

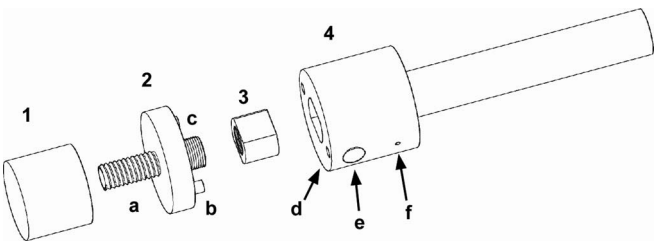

FIG. 2. Solid sorbent doser components: (1) machined cryostat mount with threaded hole, (2) agent cartridge with (a) threading to mate with the cryostat mount, (b) posts to mate with the transfer mount, (c) fine threaded hole to mate with the cap, (3) sealing cap, and (4) mounting adapter, (d) hole to mate with the cartridge, (e) press fit rare earth magnets to secure cap, (f) set screw to secure the transfer mount to the transfer arm.

2. Directional vapor doser

A second directional CWA doser that is coupled to the chamber through a stainless steel gas line and valve assembly is used for high vapor pressure liquids. Because the reservoir for this liquid source resides within the confines of the chemical fume hood, even highly toxic compounds can be dosed with this method. The reservoir is composed of a custom cartridge, which can be loaded with the liquid (typically 10–30 μL for semi-volatile compounds). The cartridge is mounted onto a multi-valve stainless steel manifold via VCR connections. Standard freeze-pump-thaw cycles are used to degas the liquid sample and remove any air remaining in the cartridge. Once the sample is purified, an evacuated heated transfer line is used to transport the vapor into the UHV chamber via a precision leak valve. On the UHV side of the leak valve, a stainless steel tube wrapped in a coiled heater (OEM)

directs the vapor toward the sample. The entire dosing manifold can be heated to high temperatures for decontamination and features redundant valves to ensure worker safety. The dosing system has successfully exposed samples to the simulants dimethyl methylphosphonate (DMMP), diisopropyl methylphosphonate (DIMP), and 2-chloroethyl ethyl sulfide (2-CEES); as well as the CWAs *RS*-propan-2-yl methylphosphonofluoridate (sarin), 3,3-dimethylbutan-2-yl methylphosphonofluoridate (soman), and bis(2-chloroethyl) sulfide (sulfur mustard). An example of the real-time uptake of sarin (dose of 0.5 μL based on pressure measurements) as studied by *in situ* FTIR is presented in Sec. III.

3. Microcapillary array doser

In addition to the CWA dosers, the system is equipped with a variable flux microcapillary array doser with similar design to other previously described systems.[45] Briefly, a vacuum manifold with known volume is backfilled to a desired pressure with the gas, as measured by a capacitance manometer (MKS Instruments). A low dead volume valve is then opened to allow the gas to flow through a calibrated 10 μm orifice and into the chamber through a customized hollow linear feedthrough (Huntington Vacuum, L-2220 series). The gas then encounters a baffle to randomize gas flow and enters the chamber as a directed beam after passing through a glass microcapillary array. The hollow feedthrough is capable of translation to bring the gas source within 1 mm of the sample surface.

E. Surface analysis: IR, XPS, and TPD

During exposure of the sample to a gas of interest, via the CWA solid sorbent doser or the *ex vacuo* vapor sources, the surface chemistry can be tracked with infrared spectroscopy. The FTIR can operate in either reflection mode, as illustrated in Fig. 1, or in transmission mode for IR transparent materials by directing the beam straight through the chamber. Infrared spectroscopy is well-suited for surface science studies because it is nondestructive, surface-sensitive, and sensitive to sub-monolayer coverages of adsorbates. Reflection-absorption infrared spectroscopy (RAIRS) has been employed for structural determination and *in situ* interrogation of reaction mechanisms of self-assembled monolayers on flat gold surfaces and the exploration of the uptake of CWA simulants on nanoparticulate materials.[21,46] In addition, many polymeric coatings, such as some paints, are sufficiently reflective to enable the use of RAIRS on these complex materials.

For RAIRS, a vacuum infrared spectrometer (Bruker Vertex 80 V, with time-resolved and step-scan capabilities) has been modified to mate with the UHV system. Specifically, radiation (SiC glowbar) is first focused ($f = 180$ mm) onto a variable aperture selection wheel that defines the spot size prior to entering into the interferometer. Upon exiting the interferometer, the beam is directed to a custom designed external optics compartment that includes an $f = 250$ mm parabolic mirror for directing the beam through a differentially pumped KBr window and focusing it onto the surface sample. The beam size at the center of the chamber is estimated to be approximately 9 mm $\times$ 6 mm. The angle of incidence for reflection from a flat surface is 86° with respect to the sample plane. After exiting the chamber through a second differentially pumped KBr window, the diverging reflected beam is then focused with an ellipsoidal mirror ($f_1/f_2 = 250/40$ mm) onto the sensor element of a liquid nitrogen-cooled mercury cadmium telluride (MCT) detector. The entire beam path is under vacuum, which is important for removing background gases from the spectra and enables spectroscopic studies in the far-IR region of the electromagnetic spectrum. In addition, high reflectivity Au-coated mirrors are employed throughout the beam path to minimize loss of photons.

Although infrared spectroscopy yields information about the vibrational frequencies of surface adsorbates, complete molecular characterization often requires complementary data such as molecular mass or elemental composition. To this end, temperature-programmed desorption (TPD) can be employed to help identify adsorbates by providing mass spectra of species that desorb from the surface sample during a post-dosing thermal ramp. In addition, kinetic analysis of TPD data can be employed to determine the activation energy for desorption of molecular adsorbates.

TPD is performed by first exposing the surface to a species of interest. During this initial exposure, RAIRS is employed to monitor surface uptake and estimate coverage. Initial dosing is typically performed at low surface temperatures where residence times are sufficient to ensure constant coverage following dosing and before thermal annealing. Following dosing, the temperature of the surface is increased by driving the sample heater with a power supply under proportional-integral-derivative control (Thermionics LPS-800-1). With the liquid nitrogen reservoir on the sample holder filled, the temperature can be ramped at a rate of 0.1 to 10 K/s with approximately $\pm$1 K precision. During the thermal ramp, IR and mass spectra (see description, below) are recorded to track desorption from the surface. Mass spectral intensity versus surface temperature represents the rate of desorption, which is governed by the surface adsorbates' activation energy for desorption. In the absence of chemical reactions, the desorption rate curves can be analyzed for flat or particulate surfaces to reveal properties about the activation energy for desorption.[47,48]

Surface elemental analysis is critical for the assignment of IR spectral peaks and identification of molecular structures from mass-resolved TPD data. Elemental analysis is accomplished in this system with x-ray photoelectron spectroscopy. The XPS system consists of a dual anode (Al$K\alpha$ and Mg$K\alpha$) x-ray source (Omicron Nanotechnology, DAR 400) and is equipped with a Z translation stage with 5° X-Y tilt for alignment with the sample. Detection of photoelectrons is achieved with an Omicron Sphera hemispherical analyzer with a five-channel electron multiplier mounted at a 45° angle relative to the x-ray source. This particular instrument is capable of providing elemental surface maps with special resolution on the order of 50 μm. In addition, the XPS is complemented by the depth-profiling capabilities provided by a differentially pumped 5 kV ion gun (Phi-Ulvac FIG-5) that is capable of

generating ions from inert and reactive gases. The ion gun is positioned to enable real-time XPS monitoring of surface species during sputtering.

F. Vapor analysis: Mass spectrometry

As products are released from the surface during reaction or parent molecules desorb from the surface during TPD, they are tracked with a doubly differentially pumped quadrupole mass spectrometer, (Extrel, MAX1000 m/z = 1–1000). Each differential stage is evacuated by a 480 L/s magnetically levitated turbomolecular pump (Edwards STP-451C), which enables up to three orders of magnitude pressure differential between the main chamber and mass spectrometer chamber during an experiment. The line-of-sight of the mass spectrometer is defined by a series of apertures that separate the differential pumping stages such that the ionizer of the QMS views a 1 cm^2 spot on the surface when the surface is located at the focal point of the main chamber. The acceptance angle of the spectrometer is 1° in polar and azimuthal angles. As indicated in the schematic, the mass spectrometer is aligned such that it views the surface during dosing and while performing IR spectroscopic measurements. In this way, changes in surface vibrational modes and concentrations during dosing can be directly correlated with the mass spectra of species desorbing from the surface at any point in time.

In addition to the differentially pumped mass spectrometer, the UHV system houses an additional mass spectrometer (Stanford Research Systems, RGA300M, residual gas analyzer) that resides in the main chamber for analysis of uptake probabilities (via the King and Wells technique[49]), which requires a non-line-of-sight detector that samples the vapor in the main chamber. In this method, an inert surface (bulk Au foil) is placed in the path of the gas source during sample exposure and the partial pressure of the gas of interest, P_i, is measured. The inert surface is then removed, exposing the sample to the gas source and the new chamber pressure, P_f, is determined. These partial pressures are proportional to the fluxes and the overall uptake probability is given by $\gamma = (P_i - P_f)/P_f$. γ is equal to the long-time sticking probability for systems in which uptake involves only adsorption. However, if uptake is mediated by chemical reactions, γ provides information about reaction probabilities. RAIRS, TPD, and XPS, in conjunction with the mass spectrometer, help to distinguish between these two cases and identify systems for which adsorption and reactions are competing channels.

III. SYSTEM PERFORMANCE: CWA UPTAKE ON SILICA NANOPARTICLES

Following extensive testing with simulants, we have studied the interactions of live CWAs with amorphous silica nanoparticles. Silica (Aerosil, 200m^2/g, 20 nm particle diameter) was chosen as the first surface to study because the adsorption of many organophosphate molecules (simulants) to silica has been previously studied, both computationally and experimentally.[41,47,48] Initial benchmark experiments with both high and low vapor pressure CWAs were used to demonstrate system performance and highlight capabilities.

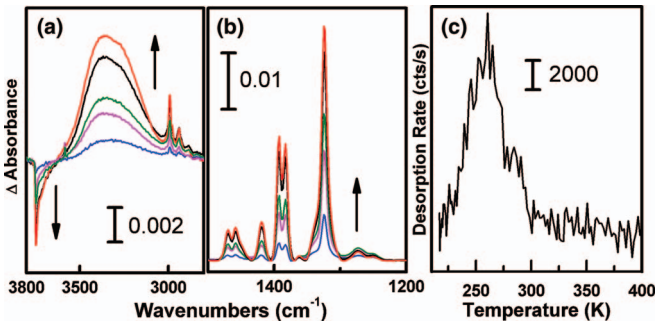

FIG. 3. (a) and (b) IR difference spectra of silica (225 K) exposed to sarin dosed with the vapor doser. The vertical bars indicate the scale in absorbance units. Arrows indicate the increase or decrease of absorbance during exposure. (c) TPD spectrum of sarin desorption from silica (ramp rate 1 K/s, monitoring mass fragment 99 amu).

(Caution: CWAs are highly toxic and should only be handled by well-trained individuals in compliance with government safety procedures and regulations.)

A. Uptake of sarin on silica

The silica sample was exposed to sarin, soman, and sulfur mustard using the vapor doser. Flux of the molecules at the surface was controlled by the precision leak valve, but maximum flux was determined by the vapor pressure of the CWA and the temperature at which the heated vapor line was maintained. Flux of soman and sarin at the surface could be controlled up to approximately 1 Langmuir/s, while for sulfur mustard the surface flux was slightly lower (~0.4 Langmuir/s). The total pressure within the chamber during the experiments was $\sim 5 \times 10^{-7}$ Torr during the dosing, otherwise the pressure was below 5×10^{-9} Torr. Agent uptake probability on silica dropped to zero after exposure to approximately 600 Langmuirs for all three CWAs.

Figures 3(a) and 3(b) show several difference IR spectra of a silica nanoparticulate surface as it is exposed to sarin. The reference spectrum for these data is that of a clean silica surface, thus any positive peaks represent new modes on the surface and negative features show modes removed from the surface. Given the density of hydroxyl groups on this sample, 2 nm^{-2} (under our sample preparation conditions), and the signal-to-noise ratio of a typical IR spectrum, we estimate that the instrument is sensitive to approximately 1% of a monolayer of adsorbates on this material. During exposure, the sharp peak at 3745 cm^{-1}, indicative of free OH groups on the surface, is converted into a broad peak at 3200 cm^{-1}, indicative of the formation of a hydrogen-bonded hydroxyl. Characteristic modes of the sarin molecule itself are also observed. These experimental results show that the uptake of sarin, and other CWAs, can be monitored with IR. Furthermore, the IR data suggest that sarin adsorbs to the surface via the same hydrogen-bonding, physisorption mechanism as previously studied organophosphorus simulants.

The strength of the sarin-silica interaction can be estimated from the change in frequency of the ν(SiO-H) mode as observed in Fig 3(a). For the common sarin simulant, dimethyl methylphosphonate (DMMP), a red shift of

601 cm^{-1} has been reported for this mode.[47] For sarin, we observe a shift of 550 cm^{-1}, suggesting that sarin interacts more weakly with the silica surface than does DMMP.

While infrared spectroscopic measurements can provide an estimate of adsorption strength, a more direct method for measuring the activation energy for desorption is temperature-programmed desorption (TPD). For TPD experiments, an adsorbate-saturated surface is heated at a constant rate and gas-phase species are detected with a mass spectrometer. For the electron-impact ionization method employed here, the signal is directly proportional to desorption rate.

Data from a typical TPD experiment for the desorption of sarin from silica are shown in Figure 3(c). As the silica surface is heated at 1 K/s, the rate of desorption increases (simple exponential dependence of the rate constant on temperature) then the rate decreases (as the surface concentration of sarin diminishes). The TPD profile obtained here is typical for first-order desorption kinetics, which is expected for molecular desorption of sarin.[47] Based on the signal to noise ratio and the coverage, we estimate that the TPD method has a detection limit of approximately 1% of a monolayer.

We note that prior to the experiments shown here with the agent sarin, we performed a control study with the simulant dimethyl methylphosphonate. For the control, we mimicked the conditions under which the results from a recently published experiment were recorded.[48] The IR spectral features and the TPD desorption profiles were indistinguishable, to within our signal-to-noise, for the two experiments.

In addition to RAIRS and TPD, XPS measurements are typically performed before and after dosing for elemental analysis and determining surface composition. XPS experiments help confirm the molecular desorption mechanism indicated by the IR data. A demonstration of typical XPS data is provided below.

B. Uptake of VX on silica

The solid sorbent doser has been employed to study the uptake of the agent, VX. While specifically designed for lower vapor pressure molecules, the solid sorbent doser has also been shown to be effective for dosing high vapor pressure molecules including the nerve agent simulant diispropyl methylphosphonate (DIMP). For VX dosing, the cartridge was packed with a graphitized carbon sorbent (Carbopack Y 60/80 Mesh) and then dosed with 20 μL of VX. While carbon was used for the VX experiments, the sorbent can easily be changed depending on the agent under investigation. Proper selection of sorbent material requires careful consideration, as it is important that the sorbent material itself is not involved in any agent chemistry. VX was dosed onto the silica surface by heating the cartridge (see Sec. II) and TPD experiments were performed to study the activation energy for desorption from the surface. Figure 4(a) shows a typical TPD spectrum for VX from silica. Comparing the TPD spectra of VX and sarin (3(b)), similar peak shapes are observed; however, the maximum rate of desorption of VX occurs at 350 K, which is nearly 100 K higher than that observed for sarin. These data suggest that VX interacts with the silica surface significantly more strongly than does sarin. Experiments are currently underway to further investigate the adsorption mechanism and potential decomposition pathways for VX on the surfaces of silica.

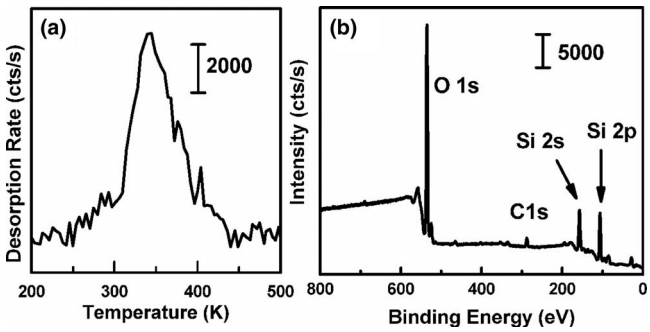

FIG. 4. (a) TPD spectrum of VX desorption from silica (ramp rate 1 K/s, mass fragment 114 amu). (b) XPS spectrum of silica following TPD of VX in which a small amount of phosphorus (~1 atomic percent) is observed.

After desorption of VX and annealing the surface to 600 K, XPS was used to search for signatures of adsorbed species that would be indicative of an irreversible chemical reaction on the surface. XPS is sensitive enough to detect below one atomic percent near the surface. Figure 4(b) shows a survey XPS scan. The small peak in the P 2p region shows that phosphorus residues remain on the silica, suggesting that, while VX desorbs molecularly at elevated temperatures (as shown in the TPD experiments), a measurable amount of decomposition on the silica surface may also occur. Future work will focus on uncovering the reaction pathways and branching ratios for this interesting system.

IV. SUMMARY

A new multifunctional UHV instrument has been successfully designed, constructed, and tested at the Edgewood Chemical and Biological Center, in Aberdeen Maryland, to perform some of the first vacuum-based surface science measurements of the interactions of CWAs with materials of interest to the military and public defense communities. Protection against the hazards of working with highly toxic compounds has been accomplished through the incorporation of a novel ventilation system and methods for directing exhaust from pumps or gases from the chamber during venting to the hood. In addition, a new doser specifically designed to enable safe, *in vacuo* dosing of low vapor pressure compounds (such as VX) was developed. All functions of the instrument were tested and evaluated during a series of experiments where the CWAs sarin, soman, sulfur mustard, and VX, as well as the simulant DIMP were dosed onto a high surface area silica surface. These experiments have been used to evaluate the type of interaction between a silica surface and gas-phase CWAs, and to determine desorption energies. Quantitative results from these measurements will be described in a forthcoming series of publications. This novel instrument will enable high-fidelity studies of the adsorption, reaction, and desorption of CWAs with surfaces of importance to national security.

ACKNOWLEDGMENTS

The authors would like to thank Dr. John Weimaster, Mr. Mark Morgan, and Dr. Chuck Bass at the Defense Threat Reduction Agency and Dr. Stephen Lee, Dr. Jennifer Becker at the Army Research Office for their support (Contract Nos. W911NF-09-1-0150 and W911NF-06-1-111, respectfully). Mr. Joseph Meyers (ECBC) is acknowledged for consultation and design and construction assistance.

[1]Y. Seto, "Decontamination of chemical and biological warfare agents," Yakugaku Zasshi **129**(1), 53–69 (2009).
[2]G. K. Prasad, P. V. R. K. Ramacharyulu, and B. Singh, "Nanomaterials based decontaminants against chemical warfare agents," J. Sci. Ind. Res. **70**(2), 91–104 (2011).
[3]S. Sundarrajan, A. R. Chandrasekaran, and S. Ramakrishna, "An update on nanomaterials-based textiles for protection and decontamination," J. Am. Ceram. Soc. **93**(12), 3955–3975 (2010).
[4]J. P. Fitch, E. Raber, and D. R. Imbro, "Technology challenges in responding to biological or chemical attacks in the civilian sector," Science **302**(5649), 1350–1354 (2003).
[5]T. Hirakawa, N. Mera, T. Sano, N. Negishi, and K. Takeuchi, "Decontamination of chemical warfare agents by photocatalysis," Yakugaku Zasshi **129**(1), 71–92 (2009).
[6]M. Houston and R. G. Hendrickson, "Decontamination," Crit. Care Clin. **21**(4), 653 (2005).
[7]E. Raber, T. M. Carlsen, K. J. Folks, R. D. Kirvel, J. I. Daniels, and K. T. Bogen, "How clean is clean enough? Recent developments in response to threats posed by chemical and biological warfare agents," Int. J. Environ. Health Res. **14**(1), 31–41 (2004).
[8]Y. C. Yang, J. A. Baker, and J. R. Ward, "Decontamination of chemical warfare agents," Chem. Rev. **92**(8), 1729–1743 (1992).
[9]L. M. Eubanks, T. J. Dickerson, and K. D. Janda, "Technological advancements for the detection of and protection against biological and chemical warfare agents," Chem. Soc. Rev. **36**(3), 458–470 (2007).
[10]R. S. Golightly, W. E. Doering, and M. J. Natan, "Surface-enhanced raman spectroscopy and homeland security: A perfect match?" ACS Nano **3**(10), 2859–2869 (2009).
[11]J. Janata, "Role of analytical chemistry in defense strategies against chemical and biological attack," Annu. Rev. Anal. Chem. **2**, 321–331 (2009).
[12]G. W. Wagner and B. K. MacIver, "Degradation and fate of mustard in soil as determined by C-13 MAS NMR," Langmuir **14**(24), 6930–6934 (1998).
[13]S. L. Bartelt-Hunt, D. R. U. Knappe, and M. A. Barlaz, "A review of chemical warfare agent simulants for the study of environmental behavior," Crit. Rev. Environ. Sci. Technol. **38**(2), 112–136 (2008).
[14]A. H. Love, A. L. Vance, J. G. Reynolds, and M. L. Davisson, "Investigating the affinities and persistence of VX nerve agent in environmental matrices," Chemosphere **57**(10), 1257–1264 (2004).
[15]N. B. Munro, S. S. Talmage, G. D. Griffin, L. C. Waters, A. P. Watson, J. F. King, and V. Hauschild, "The sources, fate, and toxicity of chemical warfare agent degradation products," Environ. Health Perspect. **107**(12), 933–974 (1999).
[16]V. M. Bermudez, "Adsorption on carbon nanotubes studied using polarization-modulated infrared reflection-absorption spectroscopy," J. Phys. Chem. B **109**(20), 9970–9979 (2005).
[17]V. M. Bermudez, "Effect of humidity on the interaction of dimethyl methylphosphonate (DMMP) vapor with SiO_2 and Al_2O_3 surfaces, studied using infrared attenuated total reflection spectroscopy," Langmuir **26**(23), 18144–18154 (2010).
[18]D. A. Chen, J. S. Ratliff, X. F. Hu, W. O. Gordon, S. D. Senanayake, and D. R. Mullins, "Dimethyl methylphosphonate decomposition on fully oxidized and partially reduced ceria thin films," Surf. Sci. **604**(5–6), 574–587 (2010).
[19]M. K. Ferguson-McPherson, E. R. Low, A. R. Esker, and J. R. Morris, "Corner capping of silsesquioxane cages by chemical warfare agent simulants," Langmuir **21**(24), 11226–11231 (2005).
[20]I. D. Gay, A. J. McFarlan, and B. A. Morrow, "Trimethyl phosphite adsorbed on silica - An NMR and infrared study," J. Phys. Chem. **95**(3), 1360–1368 (1991).
[21]W. O. Gordon, B. M. Tissue, and J. R. Morris, "Adsorption and decomposition of dimethyl methylphosphonate on Y_2O_3 nanoparticles," J. Phys. Chem. C **111**(8), 3233–3240 (2007).
[22]Y. X. Li, J. R. Schlup, and K. J. Klabunde, "Fourier-transform infrared photoacoustic-spectroscopy study of the adsorption of organophosphorus compounds on heat-treated magnesium-oxide," Langmuir **7**(7), 1394–1399 (1991).
[23]M. B. Mitchell, V. N. Sheinker, and E. A. Mintz, "Adsorption and decomposition of dimethyl methylphosphonate on metal oxides," J. Phys. Chem. B **101**(51), 11192–11203 (1997).
[24]D. Panayotov, P. Kondratyuk, and J. T. Yates, "Photooxidation of a mustard gas simulant over TiO_2-SiO_2 mixed-oxide photocatalyst: Site poisoning by oxidation products and reactivation," Langmuir **20**(9), 3674–3678 (2004).
[25]D. A. Panayotov and J. R. Morris, "Thermal decomposition of a chemical warfare agent simulant (DMMP) on TiO_2: Adsorbate reactions with lattice oxygen as studied by infrared spectroscopy," J. Phys. Chem. C **113**(35), 15684–15691 (2009).
[26]D. A. Panayotov, D. K. Paul, and J. T. Yates, "Photocatalytic oxidation of 2-chloroethyl ethyl sulfide on TiO_2-SiO_2 powders," J. Phys. Chem. B **107**(38), 10571–10575 (2003).
[27]J. S. Ratliff, S. A. Tenney, X. Hu, S. F. Conner, S. Ma, and D. A. Chen, "Decomposition of dimethyl methylphosphonate on Pt, Au, and Au-Pt clusters supported on TiO_2(110)," Langmuir **25**(1), 216–225 (2009).
[28]B. Nazari and M. Jaafari, "A new method for the synthesis of MgO nanoparticles for the destructive adsorption of organophosphorus compounds," Dig. J. Nanomater. Biostruct. **5**(4), 909–917 (2010).
[29]D. A. Panayotov and J. R. Morris, "Uptake of a chemical warfare agent simulant (DMMP) on TiO_2: Reactive adsorption and active site poisoning," Langmuir **25**(6), 3652–3658 (2009).
[30]G. S. Groenewold, G. L. Gresham, R. Avci, and M. Deliorman, "Characterization of bidentate phosphoryl compounds on soil particulates using SIMS," Surf. Interface Anal. **41**(3), 244–250 (2009).
[31]K. Kim, O. G. Tsay, D. A. Atwood, and D. G. Churchill, "Destruction and detection of chemical warfare agents," Chem. Rev. **111**(9), 5345–5403 (2011).
[32]J. Vanbokhoven, A. E. T. Kuiper, and J. Medema, "Role of heterogeneity in kinetics of a surface-reaction. 2. Kinetics of decomposition of isopropyl methylphosphonofluoridate adsorbed on gamma-alumina," Chin. J. Catal. **43**(1–3), 168–180 (1976).
[33]J. Vanbokhoven, A. E. T. Kuiper, and J. Medema, "Role of heterogeneity in kinetics of a surface-reaction. 3. Distributions in activation enthalpy and entropy," Chin. J. Catal. **43**(1–3), 181–191 (1976).
[34]A. E. T. Kuiper, J. Vanbokhoven, and J. Medema, "Role of heterogeneity in kinetics of a surface-reaction. 1. Infrared characterization of adsorption structures of organophosphonates and their decomposition," Chin. J. Catal. **43**(1–3), 154–167 (1976).
[35]O. G. Strukov, V. A. Petrunin, B. V. Sheluchenko, A. D. Kuntsevich, G. I. Drozd, and S. M. Makarochkina, "Investigation of adsorption of O-pinacolyl- and O-isopropylmethylfluorphosphonates on gamma-Al_2O_3 surface by infrared internal reflection spectroscopy," Dokl. Akad. Nauk **368**(6), 787–789 (1999).
[36]G. W. Wagner, P. W. Bartram, O. Koper, and K. J. Klabunde, "Reactions of VX, GD, and HD with nanosize MgO," J. Phys. Chem. B **103**(16), 3225–3228 (1999).
[37]G. W. Wagner and P. W. Bartram, "Reactions of VX, HD, and their simulants with NaY and AgY zeolites. Desulfurization of VX on AgY," Langmuir **15**(23), 8113–8118 (1999).
[38]G. W. Wagner, O. B. Koper, E. Lucas, S. Decker, and K. J. Klabunde, "Reactions of VX, GD, and HD with nanosize CaO: Autocatalytic dehydrohalogenation of HD," J. Phys. Chem. B **104**(21), 5118–5123 (2000).
[39]G. W. Wagner, L. R. Procell, R. J. O'Connor, S. Munavalli, C. L. Carnes, P. N. Kapoor, and K. J. Klabunde, "Reactions of VX, GB, GD, and HD with nanosize Al_2O_3. Formation of aluminophosphonates," J. Am. Chem. Soc. **123**(8), 1636–1644 (2001).
[40]A. Saxena, A. K. Srivastava, B. Singh, A. K. Gupta, M. V. S. Suryanarayana, and P. Pandey, "Kinetics of adsorptive removal of DECIP and GB on impregnated Al_2O_3 nanoparticles," J. Hazard. Mater. **175**(1–3), 795–801 (2010).
[41]D. E. Taylor, K. Runge, M. G. Cory, D. S. Burns, J. L. Vasey, J. D. Hearn, K. Griffith, and M. V. Henley, "Surface binding of organophosphates on silica: Comparing experiment and theory," J. Phys. Chem. C **117**(6), 2699–2708 (2013).
[42]S. Neatu, B. Cojocaru, V. I. Parvulescu, V. Somoghi, M. Alvaro, and H. Garcia, "Visible-light C-heteroatom bond cleavage and detoxification of chemical warfare agents using titania-supported gold nanoparticles as photocatalyst," J. Mater. Chem. **20**(20), 4050–4054 (2010).

[43]G. W. Wagner, R. J. O'Connor, J. L. Edwards, and C. A. S. Brevett, "Effect of drop size on the degradation of VX in concrete," Langmuir **20**(17), 7146–7150 (2004).
[44]G. W. Wagner, "Decontamination of chemical warfare agents using household chemicals," Ind. Eng. Chem. Res. **50**(21), 12285–12287 (2011).
[45]G. L. Fisher and C. A. Meserole, "Design for a kinematic, variable flux microcapillary array molecular beam doser," J. Vac. Sci. Technol. A **23**(4), 722–724 (2005).
[46]J. W. Lu, L. R. Fiegland, E. D. Davis, W. A. Alexander, A. Wagner, R. D. Gandour, and J. R. Morris, "Initial reaction probability and dynamics of ozone collisions with a vinyl-terminated self-assembled monolayer," J. Phys. Chem. C **115**(51), 25343–25350 (2011).
[47]A. R. Wilmsmeyer, W. O. Gordon, E. D. Davis, D. Troya, B. A. Mantooth, T. A. Lalain, and J. R. Morris, "Infrared spectra and binding energies of chemical warfare nerve agent simulants on the surface of amorphous silica," J. Phys. Chem. C **117**(30), 15685–15697 (2013).
[48]A. R. Wilmsmeyer, J. Uzarski, P. J. Barrie, and J. R. Morris, "Interactions and binding energies of dimethyl methylphosphonate and dimethyl chlorophosphate with amorphous silica," Langmuir **28**(30), 10962–10967 (2012).
[49]D. A. King and M. G. Wells, "Molecular beam investigation of adsorption kinetics on bulk metal targets: Nitrogen on tungsten," Surf. Sci. **29**, 454 (1972).